The Astrophysical Journal, 577:917–922, 2002 October 1

HIGH-RESOLUTION SPATIAL AND TIMING OBSERVATIONS OF MILLISECOND PULSAR PSR J0218+4232 WITH *CHANDRA*

L. Kuiper and W. Hermsen
Space Research Organization of the Netherlands, National Institute for Space Research, Sorbonnelaan 2, 3584 CA, Utrecht, The Netherlands

F. Verbunt
Astronomical Institute, Utrecht University, P.O. Box 80000, 3508 TA, Utrecht, The Netherlands

and

S. Ord,[1] I. Stairs,[2] and A. Lyne
University of Manchester, Jodrell Bank, Macclesfield SK11 9DL, UK
Received 2002 February 25; accepted 2002 June 3

ABSTRACT

We report on high-resolution spatial and timing results for binary millisecond pulsar PSR J0218+4232 obtained with the *Chandra* HRC-I and HRC-S in imaging mode. The subarcsecond resolution image of the HRC-I (0.08–10 keV) showed that the X-ray emission from PSR J0218+4232 is consistent with that of a point source, excluding the presence of a compact nebula with a size of about 14″ for which we had indications in *ROSAT* HRI data. The presence of a DC component is confirmed. This X-ray DC component has a softer spectrum than the pulsed emission and can be explained by emission from a heated polar cap. With our HRC-S observation, we obtained a 0.08–10 keV pulse profile with high statistics showing the well-known double-peaked morphology in more detail than before: the two pulses have broad wings, and pulsed emission appears only to be absent in a narrow phase window of width $\lesssim 0.1$. The absolute timing accuracy of ~ 200 μs makes it possible to compare for the first time in absolute phase the X-ray pulse profile with the highly structured radio profile and the high-energy γ-ray profile (0.1–1 GeV). The two X-ray pulses are aligned within absolute timing uncertainties with two of the three radio pulses. Furthermore, the two γ-ray pulses are aligned with the two nonthermal X-ray pulses, corresponding to a probability for a random occurrence of 4.9 σ, strengthening the credibility of the earlier reported first detection of pulsed high-energy γ-ray emission from this millisecond pulsar.

Subject headings: pulsars: individual (PSR J0218+4232) — X-rays: stars

1. INTRODUCTION

PSR J0218+4232 is a 2.3 ms pulsar in a 2 day orbit around a low-mass (~ 0.2 $M_\odot$) white dwarf companion (Navarro et al. 1995; van Kerkwijk 1997). Pulsed X-ray emission with a Crab-like double-pulse profile has been reported from *ROSAT* 0.1–2.4 keV data (Kuiper et al. 1998b) and *BeppoSAX* MECS 1.6–10 keV data (Mineo et al. 2000). The pulsed spectrum as measured by the MECS appeared to be remarkably hard, with a power-law photon index of 0.61 ± 0.32, harder than measured for any other radio pulsar. Furthermore, Kuiper et al. (2000) report the detection with EGRET of pulsed high-energy (0.1–1 GeV) γ-ray emission from this millisecond pulsar. Their argument is based on three lines of evidence: (1) the 0.1–1 GeV data show a 3.5 σ pulsation at the radio period; (2) the γ-ray light curve resembles the one seen in hard X-rays, namely, a phase separation of ~ 0.45 between two pulses/maxima; and (3) the spatial analysis shows that the position of the EGRET source 3EG J0222+4253 moves from the position of the nearby BL Lac 3C 66A toward the pulsar position with decreasing γ-ray energy (for energies between 100 and 300 MeV, all source counts could be attributed to PSR J0218+4232). They also showed that the two γ-ray pulses/maxima appeared to be aligned in absolute phase with two of the three radio pulses detected at 610 MHz. Unfortunately, the timing accuracies of the *ROSAT* and *BeppoSAX* observations were insufficient to construct X-ray profiles in absolute phase. None of the current models for pulsed X-ray and γ-ray emission from radio pulsars offers a consistent explanation for the above summarized high-energy results on PSR J0218+4232 (Kuiper et al. 2000).

PSR J0218+4232 is also remarkable in that it is the only Crab-like millisecond pulsar with a large DC (unpulsed) fraction of $63\% \pm 13\%$ in the *ROSAT* band below 2.4 keV (Kuiper et al. 1998b), as well as a large DC fraction of $\sim 50\%$ in radio, systematically over the range 100–1400 MHz (Navarro et al. 1995). The DC components as measured in the *ROSAT* and radio observations could be explained by emission from a compact nebula with diameter $\sim 14''$, but in both cases the indications were at the limit of the imaging capabilities. Assuming that the radio DC component is compact, combined with the measured very broad and structured radio pulse profile, Navarro et al. (1995) suggested that the magnetic field of PSR J0218+4232 is almost aligned with the rotation axis, the observer viewing the system under a small angle with respect to the rotation axis. Stairs, Thorsett, & Camilo (1999) measured the magnetic inclination angle analyzing radio polarization profiles. Their rotation vector model fits indicate that the magnetic inclination angle is indeed consistent with 0° ($8^\circ \pm 11^\circ$). Unfortunately, in their fits, the line-of-sight inclination is unconstrained. If the DC component in X-rays is also com-

[1] Current address: Center for Astrophysics and Supercomputing, Swinburne University of Technology, P.O. Box 218, Hawthorn, Victoria 3122, Australia.

[2] Current address: NRAO, P.O. Box 2, Green Bank, WV 24944.

pact, for the suggested geometry of a nearly aligned rotator and a small viewing angle, it can originate in the pulsar magnetosphere, as well as from a heated polar cap of the neutron star.

The objectives of our *Chandra* observations were (1) to establish the spatial extent of the X-ray DC component, compact or extended, and (2) to construct an X-ray pulse profile that can be compared in absolute phase with radio profiles and the 3.5 σ EGRET high-energy (0.1–1 GeV) γ-ray profile.

2. OBSERVATIONS

PSR J0218+4232 was observed with the HRC-I and HRC-S instruments on the *Chandra X-Ray Observatory* during two observations of ~75 ks duration each. The High Resolution Cameras (HRCs) are multichannel plate (MCP) detectors sensitive to X-rays in the 0.08–10 keV energy range with no spectral information.

The first observation with the HRC-I camera at the focal plane of the telescope mirror took place on 1999 December 22 for an effective exposure of 74.11 ks. Unfortunately, this observation suffered from a nonrecoverable timing ("wiring") problem incorrectly assigning the event trigger time to that of the next trigger (Tennant et al. 2001). Onboard event screening prevents recovering the true event times of all the triggers in the telemetry stream by simple backshifting. The timing accuracy in this case is determined by the total event rate, typically 300–400 s^{-1}, and is much worse than the 16 μs intrinsic timing resolution. This degradation prevents the construction of high-resolution pulse profiles in the case of millisecond pulsars.

In a reobservation of PSR J0218+4232 on 2000 October 5, for an effective exposure of 73.21 ks with the HRC-S in imaging mode (using only the central MCP segment), all event triggers could be put in the telemetry stream, so that back-shifting recovers the intrinsic timing accuracy.

3. SPATIAL ANALYSIS WITH HRC-I

PSR J0218+4232 has clearly been detected near the center of the 30′ × 30′ field of view in the 74.11 ks HRC-I observation. Within 14.′5 from the pulsar, 51 X-ray sources have been detected; some of them have counterparts in our previous *ROSAT* HRI (0.1–2.4 keV) and *BeppoSAX* MECS (1.6–10 keV) observations (Kuiper et al. 1998b; Mineo et al. 2000). The central ~7′ × 7′ part of the X-ray image containing PSR J0218+4232 has also been observed at optical wavelengths by the Keck telescope (van Kerkwijk 2001), and it turns out that all central sources except one have optical counterparts. Relative astrometry demonstrates that the *Chandra* positions are accurate to within 0.″5(1) , better than the celestial localization accuracy determination requirement of 1″. Using the standard level 1 event file provided by the *Chandra* X-Ray Center (CXC) pipeline analysis (this file contains all HRC triggers with the position information corrected for instrumental [degap] and aspect [dither] effects), a zoom-in at the pulsar location (Fig. 1, *left*) shows that the X-ray centroid has a ~0.″6 offset from the radio pulsar position of $2^h18^m6^s.351$, 42°32′17.″45 (epoch J2000), consistent with our previous findings. It is also evident from the image shown in Figure 1 (*left*) that the source events are concentrated within a circle with a radius of ~2″ from the X-ray centroid. A more quantitative estimate involves a maximum likelihood fitting of the measured two-dimensional spatial distribution with a model composed of a Gaussian and a generalized Lorentzian with free shape parameters, normalization, and centroid position on top of

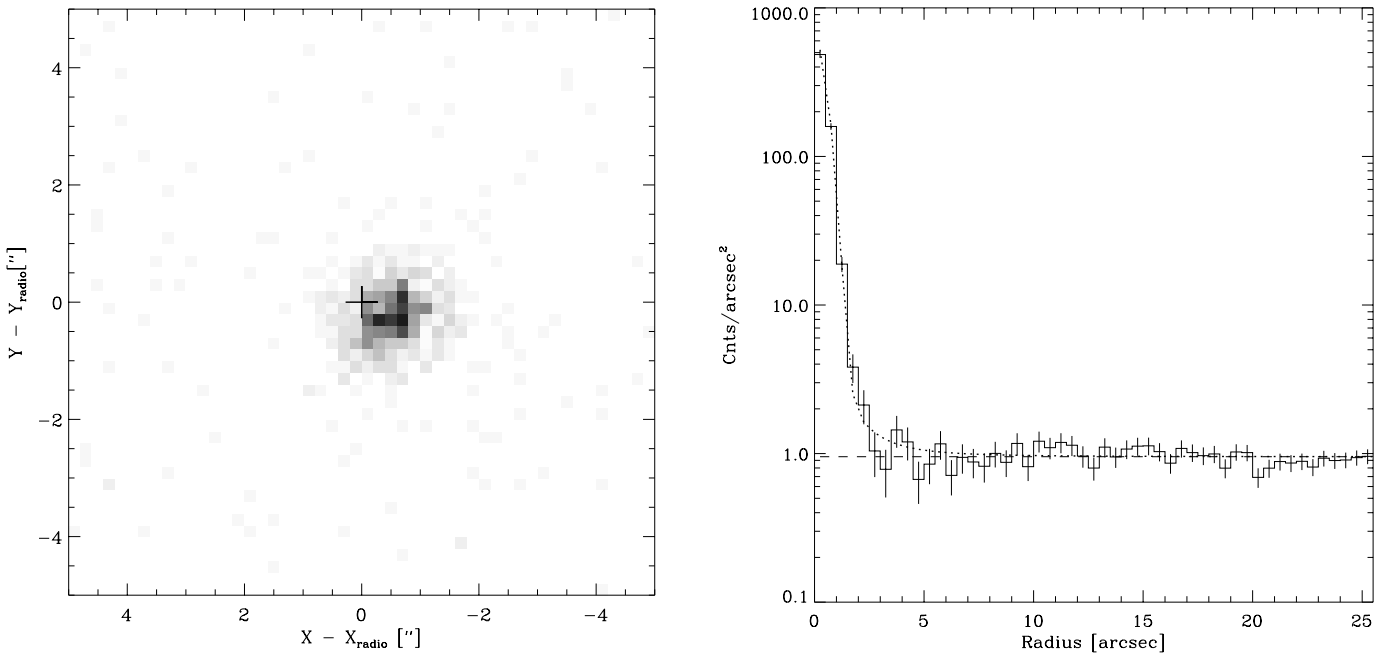

FIG. 1.—*Left*: *Chandra* 0.08–10 keV HRC-I image of a 10″ × 10″ region centered on the radio pulsar position of PSR J0218+4232. The radio position is marked with a plus sign. The angular distance between the radio pulsar position and the X-ray centroid is ~0.″6, consistent with the *Chandra* localization accuracy. *Right*: Radial distribution of HRC-I (level 1) events using the best-fit maximum likelihood X-ray position as center. Superposed as a dotted line is the radial profile from the PSF determined from the two-dimensional fit procedure, which is consistent with the *Chandra* response to a point source. The dashed line indicates the background level derived from counts in the range 10″–25″ from the center.

an (assumed) flat background, also with free scale factor. The optimum X-ray centroid position is $2^h18^m6\overset{s}{.}305(1)$, $42°32'17\overset{''}{.}23(2)$ (epoch J2000), while the radial profile of the best model fit is compatible with the point-spread function (PSF) of the High-Resolution Mirror Assembly (HRMA)/HRC-I combination (95% of the source counts are within $2''$ from the X-ray centroid). Figure 1 (*right*) shows the best model profile (*dotted line*) superposed on the measured radial profile using the optimum X-ray centroid position as center. Thus, we have no evidence for extended emission near PSR J0218+4232 at $\sim 1''$ scales (diameter), rejecting the indication for a compact nebula found in our analysis of *ROSAT* HRI data (Kuiper et al. 1998b).

The total number of counts assigned to the pulsar from the maximum likelihood fit is 870 ± 30, which translates to a count rate of $(1.175 \pm 0.041) \times 10^{-2}$. Assuming absorption in a column with density $N_H = 5 \times 10^{20}$ cm^{-2} (Verbunt et al. 1996) and a photon power-law index of 0.94 (Mineo et al. 2000), the count rate converts to a 2–10 keV flux of $(5.2 \pm 0.2^{+2.1}_{-1.3}) \times 10^{-13}$ ergs cm^{-2} s^{-1}. The first error represents the statistical error and the second the systematic error due to uncertainties in the absolute sensitivity of the HRC-I and in the spectral model. The value is consistent with the *BeppoSAX* MECS value of $(4.38 \pm 0.48 \pm 0.44) \times 10^{-13}$ ergs cm^{-2} s^{-1} (the first error represents the statistical uncertainty and the second error the systematic uncertainty of about 10%).

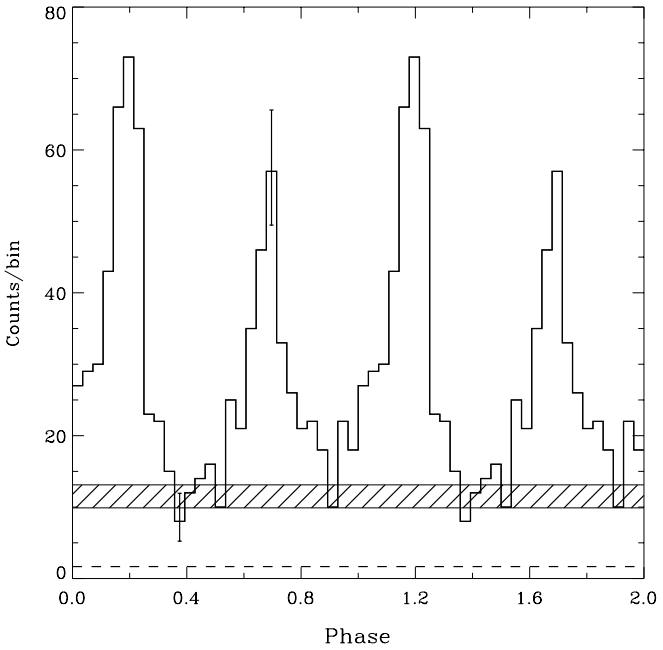

FIG. 2.—Pulse profile of PSR J0218+4232 as measured by the HRC-S in imaging mode. Two cycles are shown for clarity. Typical error bars are shown at phases 0.35 and 0.7. The DC level ($\pm 1\ \sigma$) is indicated by the hatched area, and the background level from the imaging analysis by the dashed line.

4. TIMING ANALYSIS WITH HRC-S

In a spatial analysis using the HRC-S level 1 event file, the X-ray centroid of the X-ray counterpart of PSR J0218+4232 was found to have an offset of $1\overset{''}{.}9$ from the radio position of the pulsar, larger than the celestial location accuracy determination requirement of $1''$; a systematic difference noticed earlier by, e.g., Wang et al. (2001). The number of counts assigned to the source, applying a similar likelihood procedure as in the case of the HRC-I image data, is 755 ± 28. Using the optimized background scale factor and source profile, the optimum radius for event extraction (signal-to-noise ratio [S/N] optimal) from the best-fit centroid turns out to be $1\overset{''}{.}5$.

The first step in the timing analysis is to correct the assigned event times by backshifting, recovering the intrinsic relative time resolution of 16 μs. Next, the event extraction radius was set to the optimum radius of $1\overset{''}{.}5$. The final step is the determination of the arrival times at the solar system barycenter using the orbital information of *Chandra* and the position of PSR J0218+4232. Folding the barycentered arrival times with the spin and binary parameters from an updated ephemeris for PSR J0218+4232 revealed the well-known double-peaked profile at high statistics (Fig. 2). The deviation from a flat distribution is 15.2 σ according to a Z_6^2-test, and the peak separation is 0.475 ± 0.015, consistent with previous estimates (Kuiper et al. 1998b; Mineo et al. 2000). The peak widths $\Delta\phi$ (FWHM), fitting the profile in terms of two asymmetric Lorentzians atop a flat background, are Peak-1 (at $\phi \simeq 0.2$) 0.116 ± 0.019 (267 ± 44 μs) and Peak-2 (at $\phi \simeq 0.7$) 0.109 ± 0.025 (251 ± 58 μs). Fitting two Gaussians plus background yielded similar results.

In Figure 2 is indicated an estimate for the unpulsed (DC) level ($\pm 1\ \sigma$) using a bootstrap method outlined by Swanepoel, de Beer, & Loots (1996). Furthermore, the background level estimated in the maximum likelihood imaging analysis is also shown, giving a number of background counts within the $1\overset{''}{.}5$ extraction radius of (46.9 ± 0.4). The pointlike (see § 3) DC (unpulsed) component, significantly detected with *ROSAT* (0.1–2.4 keV; 4.8 σ) by Kuiper et al. (1998b) and weakly with *BeppoSAX* (1.6–4.0 keV; $\sim 2\ \sigma$) by Mineo et al. (2000) is clearly seen in this 0.08–10 keV profile. The pulsed fraction F_P, defined as $N_P/(N_P + N_{DC})$, where N_P specifies the number of pulsed source counts and N_{DC} the number of DC source counts, turns out to be $F_P = 0.64 \pm 0.06$, as measured by *Chandra* HRC-S over the entire 0.08–10 keV energy range.

Finally, our *Chandra* HRC-S 0.08–10 keV X-ray pulse profile can be directly compared in absolute phase with our previously derived radio and γ-ray profiles (Kuiper et al. 2000); first, because we generated an ephemeris valid for all used observation periods and applied a common reference epoch (see Table 1), and second, because the absolute timing accuracy of *Chandra* is within 200 μs (Tennant et al. 2001), which corresponds to a phase inaccuracy smaller than 0.085, given the pulse period of 2.3 ms. Figure 3 shows then for the first time the comparison of a PSR J0218+4232 X-ray profile in absolute phase with the radio and γ-ray profiles. Within the uncertainties of each of the measurements, the X-ray pulses are aligned with two of the three radio pulses at 610 MHz and with the γ-ray pulses.

5. *CHANDRA* HRC-S X-RAY PULSE PROFILE VERSUS EGRET HIGH-ENERGY γ-RAY PROFILE

The alignment in absolute phase of the very hard X-ray pulses with the low-significance γ-ray pulses is particularly interesting. The calculated 3.5 σ significance of the γ-ray profile was derived for *unbinned* data, giving the statistical evidence (Z_4^2-test) for deviations from a flat distribution

TABLE 1
EPHEMERIS OF PSR J0218+4232 BASED ON RADIO TIMING MEASUREMENTS SPREAD OVER A 6.5 yr PERIOD

Parameter	Value
Right ascension (J2000)	$02^h18^m6^s.351$
Declination (J2000)	$42°32'17''.45$
Epoch validity start/end (MJD)	49092–51462
Frequency	430.4610670731491 Hz
Frequency derivative	-1.43397×10^{-14} Hz s^{-1}
Epoch of the period (MJD)	50277.000000025
Orbital period	175292.302218 s
$a \sin i$	1.9844301 (lt-s)
Eccentricity	0
Longitude of periastron	0
Time of ascending node (MJD)	50276.61839862
rms of timing solution	14.4 milliperiods; 33.4 μs

anywhere in the pulsar phase. When we calculate the significance of detection of the two γ-ray pulses at the *known* absolute phases of the X-ray pulses (e.g., by determining the pulsed excess counts in the narrow pulse phase windows 0.10–0.30 and 0.55–0.70, considering the remaining phase windows [65%] as background; we found 54.8 ± 13.7 pulsed excess counts), then we derive for this single trial an increased total significance of 4.0 σ.

In fact, we performed simulations similar to what we did earlier for PSR B1951+32 (Kuiper et al. 1998a): we simulated 10^6 flat phase distributions with the same number of counts ($n = 308$) as contained in the EGRET 0.1–1 GeV phase histogram shown in Figure 3*c*. Then we applied the Z_4^2-test and verified first that the distribution of the Z_4^2 simulations behaved as expected for a random distribution (with 10^6 trials we could calibrate well up to $\sim$4.5 σ). Next, we used again the two narrow pulse phase windows 0.10–0.20 and 0.55–0.70 to determine the pulsed excess counts. Figure 4 shows in a two-dimensional distribution all simulations with a Z_4^2-significance above 3 σ versus the measured pulsed excess counts in the predefined pulse windows. As can be seen, only for one simulation out of 10^6 a significance above 3.5 σ *and* pulsed excess counts above 55 was reached. This corresponds to a statistical significance of $\sim$4.9 σ. Therefore, we take the alignment in absolute phase of the nonthermal X-ray and γ-ray pulses as supporting evidence for our first detection of high-energy γ-rays from a millisecond pulsar.

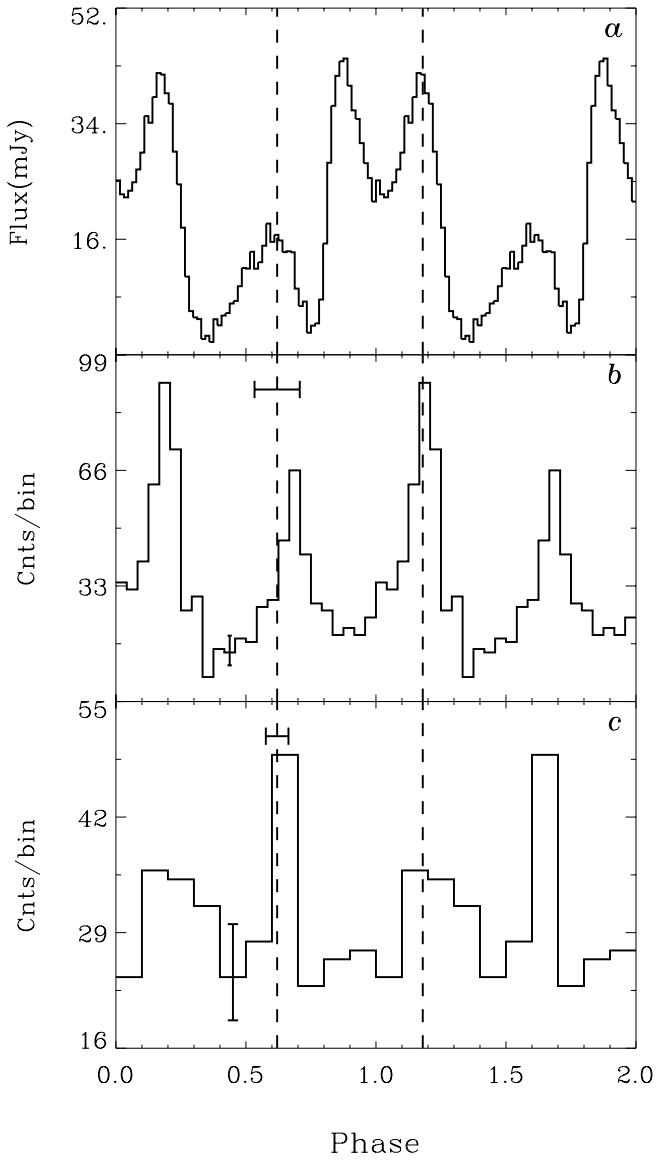

FIG. 3.—Multiwavelength pulse profiles of PSR J0218+4232 in absolute phase. (*a*) Radio pulse profile at 610 MHz. (*b*) *Chandra* HRC-S X-ray pulse profile (0.08–10 keV; timing accuracy 200 μs or 0.085 in phase). (*c*) EGRET γ-ray pulse profile (0.1–1 GeV; timing accuracy 100 μs or 0.043 in phase). The absolute timing accuracies of the X-ray and γ-ray profiles are shown as horizontal bars centered on phase 0.62. Indicated by dotted lines are the positions of the two pulses in the 610 MHz radio profile that coincide with the high-energy pulses. Typical ± 1 σ error bars are indicated in the X-ray and γ-ray profiles. Note that the background level in the γ-ray profile as determined from an imaging analysis is at 22.2 (Kuiper et al. 2000).

6. SPECTRAL ANALYSIS

In the spatial and timing analyses, we derived the main results from our *Chandra* data, which contain very limited spectral information. Essentially, we measured the integral count rate over the entire 0.08–10 keV energy window. Therefore, we cannot add significant new information to the well-defined pulsed spectrum as measured by the *BeppoSAX* MECS instrument (Mineo et al. 2000). However, no meaningful information has been published so far on the spectral shape of the DC component (crucial to decide on the origin and production mechanism), while the combined *ROSAT* HRI, *BeppoSAX* MECS, and *Chandra* data can give a first estimate: the *ROSAT* HRI provides us with a DC count rate for 0.1–2.4 keV, the MECS for 1.6–4 keV and 4–10 keV, and *Chandra* for 0.08–10 keV.

Assuming a spectral model and absorbing column N_H and using the instrument sensitivity curves over the different energy windows, the HRC-S DC count rate can be used to predict the *ROSAT* HRI and *BeppoSAX* MECS DC count rates.

For a blackbody model, the measured *ROSAT* HRI/HRC-S rates demand a temperature $kT \lesssim 0.9$ keV; the measured *BeppoSAX* MECS/HRC-S rates $0.5 \lesssim kT \lesssim 1.05$ (1 σ limits). Therefore, a thermal model with a temperature $0.5 \lesssim kT \lesssim 0.9$ (90% confidence interval; 0.33–1.1 keV) is consistent with all the measured DC count rates. Assuming a power-law model, the DC rates of the three instruments are consistent with power-law indices in the range 1.3–1.85

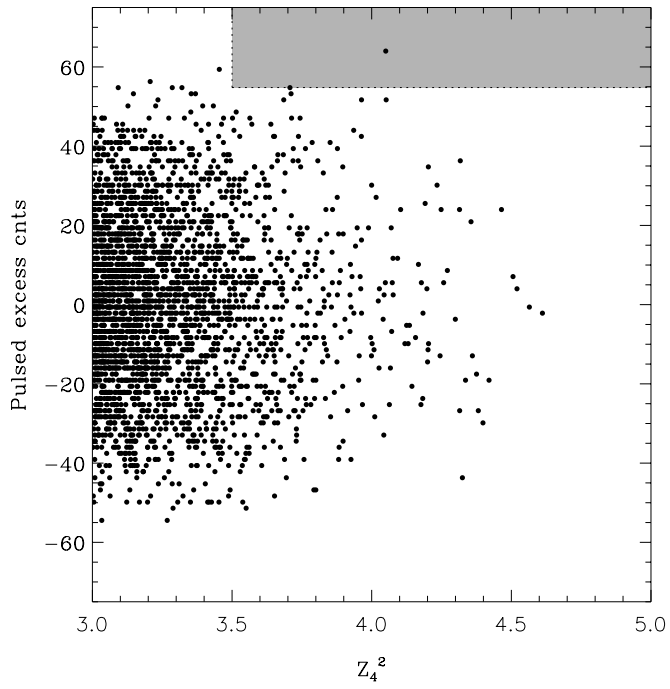

FIG. 4.—Scatter plot of pulsed excess counts vs. Z_4^2 for 10^6 background simulations. The hatched band indicates the parameter space of interest, namely, to detect by chance a signal with a modulation significance above 3.5 σ *and* more than 55 pulsed excess counts in the pulse phase windows 0.1–0.3 and 0.55–0.7 (representative for the 0.1–1 GeV γ-ray profile). We found just one occurrence in 10^6 trials, corresponding to a statistical significance of $\sim$4.9 σ.

(1 σ limits; 90% confidence interval; 0.95–2.45), significantly softer than for the pulsed emission (0.61 ± 0.32) as measured by the MECS (Mineo et al. 2000). The total statistics of the data are insufficient to discriminate between the blackbody and the power-law spectral shapes.

7. DISCUSSION AND CONCLUSIONS

Our first objective of the *Chandra* observations was to determine the spatial extent of the X-ray DC component and to find a likely explanation for its origin. As is shown in Figure 1, no evidence for extended emission near PSR J0218+4232 at $\sim 1''$ scales (diameter) is seen, rejecting the indication for a compact nebula found in our analysis of *ROSAT* HRI data (Kuiper et al. 1998b). The combined *ROSAT*, *BeppoSAX* MECS, and *Chandra* data led us to conclude that the DC spectrum is significantly softer than the pulsed spectrum, the latter being clearly of nonthermal origin. If we adopt the geometry proposed by Navarro et al. (1995), a nearly aligned rotator and a small viewing angle, the soft DC X-ray component can be explained as thermal emission from the polar cap of the neutron star that stays visible to the observer all the time. For old millisecond pulsars, the thermal emission can only originate from reheating of the polar cap area by backflowing accelerated particles. In fact, for a millisecond pulsar, the polar cap half-angle $\theta_{\rm pc}\{= \arcsin[(R_{\rm NS}2\pi/{\rm pc})^{1/2}]\}$ extends over a relatively large angle, e.g., 17°.5 for PSR J0218+4232. This means that the spin axis is well within the (magnetic) polar cap region, for the measured angle between the spin and magnetic axes amounts to $\sim 10^\circ$ ($8^\circ \pm 11^\circ$) (Stairs et al. 1999). Therefore, a small observer viewing angle to the system (angle spin axis and line of sight) can keep the observer looking at the heated polar region continuously.

The Navarro et al. (1995) radio observations had a Very Large Array (VLA) beam size of $16''$, also allowing an interpretation of the radio DC component (reported DC fraction $\sim$50%) as a compact nebula up to the size of the VLA beam. No new observations have been reported with a smaller beam size, but Stairs et al. (1999) and Kuzmin & Losovsky (2001) revisited the pulsed emission. We fitted the total radio spectrum of Navarro et al. (1995; five data points) with a power-law shape, index 2.57 ± 0.07, and the new total pulsed radio spectrum (three data points from Navarro et al. 1995, two from Stairs et al. 1999, and one from Kuzmin & Losovsky 2001), index 2.58 ± 0.15. The spectra appeared identical in shape, and the updated DC fraction is $13\% \pm 9\%$, significantly lower than the earlier estimate. This leads us to the conclusion that the radio DC component is most likely also compact and has the same magnetospheric origin as the pulsed emission, which has a very structured and remarkably broad profile and is indeed practically never "off."

Our second objective was to obtain with *Chandra* a more significant X-ray profile than measured so far, to study the profile structure in more detail in the X-ray band below 10 keV, and to have for the first time absolute timing, allowing multiwavelength phase comparisons. The profile in Figure 2 with a significance of 15.2 σ is indeed much more significant than the MECS profile (6.8 σ). Now we can really see that the two pulses have broad wings and that the profile reaches the DC level only in a very narrow phase interval around phase 0.35 (phase extent $\lesssim$0.1). In fact, Figure 3 shows that the radio and the X-ray profiles both reach a minimum level for approximately the same *absolute* phase region. Furthermore, Figure 3 shows that the X-ray pulses are aligned in absolute phase with two of the three radio pulses and the two γ-ray pulses within the timing uncertainties of the different measurements.

PSR J0218+4232 is the first and only millisecond pulsar for which we reported evidence for detection of high-energy γ-ray emission up to 1 GeV (Kuiper et al. 2000). We take the alignment in absolute phase of the nonthermal X-ray and γ-ray pulses as important supporting evidence for our first detection of high-energy γ-rays from a millisecond pulsar. In § 5, we showed that the probability that a random timing signal reaches a 3.5 σ modulation significance *and* has its 55 pulsed excess counts in phase with the two X-ray pulses amounts to $\sim$4.9 σ.

Wallace et al. (2000) reported the detection of short-term variability in the high-energy γ-ray emission from 3EG J0222+4253 (3C 66A/PSR J0218+4232) in a systematic search for all 170 unidentified sources in the Third EGRET Catalog (Hartman et al. 1999). They noted that if this flaring is due to PSR J0218+4232, "It would be an unusual source in two ways: it would be the only millisecond pulsar seen by EGRET and the only pulsar to show strong flaring." We argue, however, that in their search the reported evidence for flaring is not significant: for each of the 170 unidentified sources, Wallace et al. (2000) produced light curves per viewing period (VP) with 2 day flux values each time they were in the field of view during a VP. For 3EG J0222+4253 (3C 66A/PSR J0218+4232), they found the most significant evidence for variability, namely, in VP15 with a variability index $V = 2.6$, corresponding to a $\sim$3 σ significance for a

random detection in a *single* trial assuming Gaussian statistics (although Poisson statistics apply). This variability was due to one single high 2 day flux value. However, this source was viewed in four observations (no indication for variability in the other VPs), which makes the probability (4×0.002512) 1% or 2.58 σ to find $V = 2.6$ in one out of four observations. Furthermore, Wallace et al. (2000) analyzed 144 VPs with durations longer than 3 days, producing for the 170 unidentified sources a few hundred light curves, making the probability to find once $V = 2.6$ (or one single high 2 day flux value) few times unity! They correctly noted that their Monte Carlo probabilities give misleading values (too optimistic) as the used averages having no uncertainties assigned. Also, in the latter case, the very large number of "trials" has been ignored. Since there was no a priori reason to select 3EG J0222+4253 for a single trial, we do not regard the indication for short-term variability of this source as significant.

The X-ray results on the DC emission and the radio results on the DC and pulsed emission suggest for PSR J0218+4232 an emission scenario of a nearly aligned rotator and a small viewing angle. The latter angle can still be as large as $\sim 20^\circ$ to explain the X-ray DC emission if this originates from a polar cap heated by particle bombardment. For explaining the pulse profile with two hard-spectrum X-ray/γ-ray peaks, it is more critical to know this viewing angle to get a handle on the geometry. For both competing classes of models, polar cap models (PC; e.g., Daugherty & Harding 1994, 1996) and outer gap models (OG; see, e.g., Cheng et al. 1986a, 1986b; Ho 1989), production of hard X-ray/γ-ray emission in the magnetospheres of millisecond pulsars has been predicted (e.g., Bhattacharya & Srinivasan 1991; Sturner & Dermer 1994). Recently, millisecond pulsars, among them PSR J0218+4232, were considered for PC models by Dyks & Rudak (1999), Bulik & Rudak (1999), Bulik, Rudak, & Dyks (2000), and Zhang & Harding (2000). For PSR J0218+4232, they did not succeed in reproducing the measured high-energy spectral shape. More recently, Dyks & Rudak (2002) succeeded in reproducing the high-energy spectrum of PSR J0218+4232, but required nonorthodox assumptions about the electron energy distribution or emission altitude as well as off-beam viewing geometry. Woźna et al. (2002) reproduced the double-peak profile with the measured phase separation for a small inclination angle of 8° and a viewing angle of 29° (angles approximately consistent with our findings). However, for these angles the spectrum reached its maximum luminosity for too high energies around 100 GeV. The fact that in the case of PC models a double-peak hard X-ray/γ-ray profile can be modeled for a nearly aligned rotator with a $\sim 20^\circ$ viewing angle follows already from Daugherty & Harding (1996), who showed that the γ-ray beam produced at the polar cap rim is relatively wide, amounting to $\sim 26^\circ$ ($1.5 \times \theta_{\rm pc}$) for PSR J0218+4232. For emission produced at higher altitudes in the magnetosphere (as is proposed in the more recent versions of PC models), the beam will become even wider. In all these discussions, the real viewing angle in combination with the inclination angle determines whether the measured double-peak profile can be obtained. Also, for OG models, a double-peak profile is in principle possible, depending on the actual viewing angle and which part of the OG (in altitude) is visible to the observer. For OG models, the hard X-ray/γ-ray cone might become too broad for the case of PSR J0218+4232 as a nearly aligned rotator if the hard X-ray/γ-ray production takes place only close to the light cylinder. However, Hirotani et al. (2002) argued recently that the γ-ray production is not limited to regions in the OG above the null charge surface but can also originate from altitudes closer to the neutron star. More detailed model calculations are required to solve the present uncertainties in the overall interpretation of the data.

This underlines the importance of a new attempt to determine the geometry from radio polarization data. Then, detailed model calculations starting from this geometry can attempt to reproduce all the remarkable timing and spectral results obtained for this millisecond pulsar.

REFERENCES

Bhattacharya, D., & Srinivasan, G. 1991, J. Astrophys. Astron., 12, 17
Bulik, T., & Rudak, B. 1999, Astrophys. Lett. Commun., 38, 37
Bulik, T., Rudak, B., & Dyks, J. 2000, MNRAS, 317, 97
Cheng, K. S., Ho, C., & Ruderman, M. 1986a, ApJ, 300, 500
———. 1986b, ApJ, 300, 522
Daugherty, J. K., & Harding, A. K. 1994, ApJ, 429, 325
———. 1996, ApJ, 458, 278
Dyks, J., & Rudak, B. 1999, Astrophys. Lett. Commun., 38, 41
———. 2002, Proc. of the XXII Moriond Astrophysics Meeting, ed. A. Goldwurm, D. Neumann, & J. Tran Thanh Van (Hanoi: Gioi) (astro-ph/0205222v1)
Hartman, R. C., et al. 1999, ApJS, 123, 79
Hirotani, K., et al. 2002, Proc. of the XXII Moriond Astrophysics Meeting, ed. A. Goldwurm, D. Neumann, & J. Tran Thanh Van (Hanoi: Gioi)
Ho, C. 1989, ApJ, 342, 396
Kuiper, L., Hermsen, W., Bennett, K., Carramiñana, A., Lyne, A., McConnell, M., & Schönfelder, V. 1998a, A&A, 337, 421
Kuiper, L., Hermsen, W., Verbunt, F., & Belloni, T. 1998b, A&A, 336, 545
Kuiper, L., Hermsen, W., Verbunt, F., Thompson, D. J., Stairs, I. H., Lyne, A. G., Strickman, M. S., & Cusumano, G. 2000, A&A, 359, 615
Kuzmin, A. D., & Losovsky, B. Ya. 2001, A&A, 368, 230
Mineo, T., et al. 2000, A&A, 355, 1053
Navarro, J., de Bruyn, A. G., Frail, D. A., Kulkarni, S. R., & Lyne, A. G. 1995, ApJ, 455, L55
Stairs, I. H., Thorsett, S. E., & Camilo, F. 1999, ApJS, 123, 627
Sturner, S. J., & Dermer, C. D. 1994, A&A, 281, L101
Swanepoel, J. W. H., de Beer, C. F., & Loots, H. 1996, ApJ, 467, 261
Tennant, A. F., et al. 2001, ApJ, 554, L173
van Kerkwijk, M. 1996, in IAU Colloq. 160, Pulsars: Problems and Progress, ed. S. Johnston, M. A. Walker, & M. Bailes (San Francisco: ASP), 489
Verbunt, F., Kuiper, L., Belloni, T., Johnston, H. M., de Bruyn, A. G., Hermsen, W., & van der Klis, M. 1996, A&A, 311, L9
Wallace, P. M., et al. 2000, ApJ, 540, 184
Wang, Q. D., Gotthelf, E. V., Chu, Y.-H., & Dickel, J. R. 2001, ApJ, 559, 275
Woźna, A., Dyks, J., Bulik, T., & Rudak, B. 2002, Proc. of the XXII Moriond Astrophysics Meeting, ed. A. Goldwurm, D. Neumann, & J. Tran Thanh Van (Hanoi: Gioi) (astro-ph/0205224v1)
Zhang, B., & Harding, A. 2000, ApJ, 532, 1150